Astronomy & Astrophysics

Influence of a new potential energy surface on the rotational (de)excitation of H_2O by H_2 at low temperature

M.-L. Dubernet[1], F. Daniel[1], A. Grosjean[2], A. Faure[3], P. Valiron[3], M. Wernli[3], L. Wiesenfeld[3], C. Rist[3], J. Noga[4], and J. Tennyson[5]

[1] Observatoire de Paris-Meudon, LERMA UMR CNRS 8112, 5 Place Jules Janssen, 92195 Meudon Cedex, France
   e-mail: marie-lise.dubernet@obspm.fr
[2] Laboratoire d'Astrophysique, Observatoire de Besançon, UMR CNRS 6091, Université de Franche-Comté,
   41 bis avenue de l'Observatoire, BP 1615, 25010 Besançon Cedex, France
[3] Laboratoire d'Astrophysique, Observatoire de Grenoble, UMR CNRS 5571, Université Joseph Fourier, 38041 Grenoble Cedex 09,
   France
[4] Department of Physical and Theoretical Chemistry, Faculty of Natural Sciences, Comenius University, Mlynska dolina CH1,
   84215 Bratislava, Slovakia
[5] Department of Physics and Astronomy, University College London, Gower Street, London WC1E 6BT, UK

ABSTRACT

Aims. Using a newly determined 5D potential energy surface for H_2–H_2O we provide an extended and revised set of rate coefficients for de-excitation of the lowest 10 para- and 10 ortho- rotational levels of H_2O by collisions with para-($j = 0$) and ortho-$H_2(j = 1)$, for kinetic temperatures from 5 K to 20 K.
Methods. Our close coupling scattering calculations involve a slightly improved set of coupled channels with respect to previous calculations. In addition, we discuss the influence of several features of this new 5D interaction on the rotational excitation cross sections.
Results. The new interaction potential leads to significantly different rate coefficients for collisions with para-H_2 ($j = 0$). In particular the de-excitation rate coefficient for the 1_{10} to 1_{01} transition is increased by up to 300% at 5 K. At 20 K this increase is 75%. Rate coefficients for collisions with ortho-$H_2(j = 1)$ are modified to a lesser extent, by up to 40%. The influence of the new potential on collisions with both para-($j = 0$) and ortho-$H_2(j = 1)$ is expected to become less pronounced at higher temperatures.

Key words. molecular data – molecular processes – ISM: molecules

1. Introduction

Water is a key molecule for the chemistry and the energy balance of the gas in cold clouds and star forming regions, thanks to its relatively large abundance and large dipole moment. A wealth of observational data has already been obtained by the Infrared Space Observatory (see for example: Cernicharo et al. 2006; Cernicharo & Crovisier 2005; Spinoglio et al. 2001; Tsuji 2001; Wright et al. 2000), the Submillimeter Wave Astronomy Satellite (Melnick et al. 2000) and the ODIN satellite (Sandqvist et al. 2003; Wilson et al. 2003). In the near future the Heterodyne Instrument for the Far-Infrared (HIFI) will be launched on board the Herschel Space Observatory. It will observe with unprecedented sensitivity spectra of many molecules with an emphasis on water lines in regions from cold molecular clouds to star forming regions. The interpretation of these spectra will rely upon the accuracy of the available collisional excitation rate coefficients that enter into the population balance of the emitting levels of the molecules. In temperature range from 5 K to 1500 K the most abundant collider likely to excite the molecules is the hydrogen molecule, followed by the helium atom. In diffuse clouds and photo-ionized environments, water collisions with atomic H and electrons might also play a significant role. Much work has dealt with the rotational or ro-vibrational excitation of many molecules by He or H_2, always trying to improve accuracy

(see bibliography in the BASECOL database, Dubernet et al. 2006). Some of the latest calculations (Daniel et al. 2004; Daniel et al. 2005b; Dubernet 2005; Lique et al. 2005) have been used to model astrophysical observations and have shown that careful calculation of the excitation rate coefficients can influence the interpretation of spectra (Daniel et al. 2006, 2005a; Lique & Cernicharo 2006).

Until recently, only calculation of the excitation of water by He was feasible and a series of such calculations were performed in order to determine accurate rate coefficients (Green 1980; Palma et al. 1988b,a, 1989; Maluendes et al. 1992; Green et al. 1993). These studies involved improving the potential energy surface (PES), improving the quality of the scattering calculations and extending previous work either to a larger ranges of temperature or to more transitions.

A pioneering rigid-body 5D PES was obtained by Phillips et al. (1994) for the excitation of the rotational levels of H_2O by H_2. Using this PES, Phillips et al. (1996) computed rate coefficients for temperatures ranging from 20 K to 140 K. Dubernet & Grosjean (2002) and Grosjean et al. (2003) extended this work down to 5 K and pointed out that such low temperature rates are highly sensitive to a proper description of resonances.

Recently an accurate 9D PES for the deformable H_2–H_2O system was calculated by Faure et al. (2005a). This PES combined a) conventional 5D and 9D CCSD(T) calculations

(coupled cluster with perturbative triples), and b) accurate calibration data using the explicitly correlated CCSD(T)-R12 approach (Noga & Kutzelnigg 1994).

As a first application of the 9D PES, high temperature ($1500 < T < 4000$ K) rate constants for the relaxation of the ν_2 bending mode of H_2O were estimated from quasi classical trajectory calculations (Faure et al. 2005a) and the role of rotation in the vibrational relaxation of water was emphasized (Faure et al. 2005b).

Another application of this 9D PES was to construct an accurate 5D PES suitable for inelastic rotational calculations by averaging over H_2 and H_2O ground state vibrational states. As was pointed out in Faure et al. (2005a), this state-averaged PES is very close to a rigid-body PES using state-averaged geometries for H_2O and H_2.

A goal of this paper is to assess the influence of this new 5D PES on the rotational excitation cross sections. The composite nature of the PES also offers an opportunity to discuss the respective importance of the proper state-averaging (or of the proper choice of a rigid-body geometry) and of the R12 corrections towards the CCSD(T) infinite basis set limit.

A second goal is to use the new 5D PES of Faure et al. (2005a) to provide an extended set of rate coefficients between 5 K and 20 K for de-excitation of the lowest 10 para- and 10 ortho- rotational levels of H_2O by collisions with para-($j = 0$) and ortho-H_2($j = 1$). This set includes more rotational transitions than studied by Dubernet & Grosjean (2002) and Grosjean et al. (2003) with the rigid 5D potential energy surface of Phillips et al. (1994). The present calculations therefore use a larger rotational basis set for water in order to ensure convergence for transitions among the highest rotational levels. Another advance on previous calculations (Dubernet & Grosjean 2002; Grosjean et al. 2003; Phillips et al. 1996) is the use of experimental rotational energies (Dabrowski 1984) for the H_2 monomer. Non-equilibrium H_2 ortho-to-para ratios are observed in astrophysics so that the rate coefficients for excitation by ortho-H_2($j = 1$) could be of relevance at temperatures as low as 20 K.

Such highly accurate quantum scattering calculations are extremely computer-time consuming above 20 K. Therefore we present results now in order to make them available to the astronomical community in a timely manner. In the 5 K to 20 K range, contributions from the excited rotational states of H_2 are negligible and it is therefore computationally tractable to use both the best converged basis set and the highest accuracy scattering method. Moreover, the influence of the new PES is expected to be most significant in this low temperature range.

In Sect. 2 we make comparaisons to show the effects of the new PES and in Sect. 3 we describe our methods and present our new results.

2. Influence of the new 5D potential energy surface

Phillips et al. (1994) calculated the interaction potential for 722 points on the surface and for fixed theoretical equilibrium geometries $r_{HH} = 1.402\ a_0$, $r_{OH} = 1.809\ a_0$ and HOH angle equal to $104.52°$. The PES was obtained by means of fourth-order pertubation theory (MP4) and was expanded over 48 angular terms. Faure et al. (2005a) followed a three-step procedure: (i) a 5D rigid-rotor PES reference was computed at the CCSD(T) level of theory for fixed theoretical equilibrium geometries $r_{HH} = 1.400\ a_0$, $r_{OH} = 1.809\ a_0$ and HOH angle equal to $104.22°$; (ii) this reference surface was then calibrated to a few cm^{-1} accuracy using 812 "high cost" CCSD(T)-R12 calculations; (iii) the R12-corrected rigid rotor surface was then
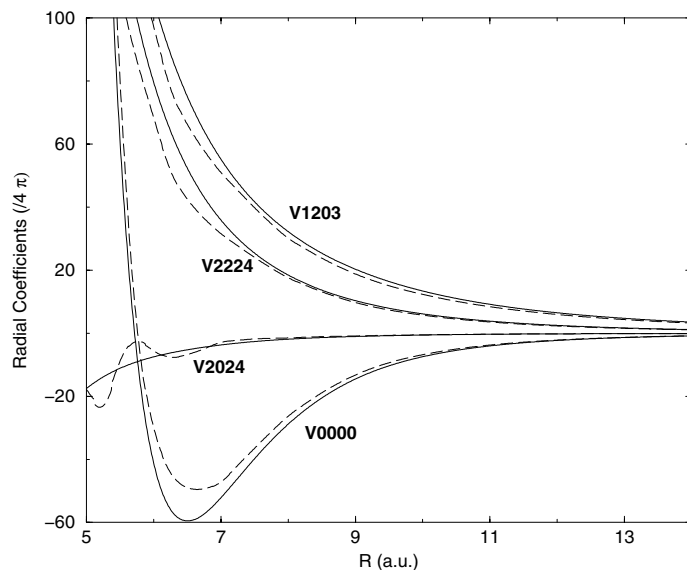

Fig. 1. Comparison of the leading radial coefficients (in cm^{-1}) of the H_2O–H_2 interaction, i.e. the isotropic term, the dipole-quadrupole term V_{1023}, the quadrupole-quadrupole terms V_{2024}, V_{2224}, from Phillips et al. (1994) (dashed lines) with the corresponding terms from the PES of Faure et al. (2005a) (solid lines) used in the present calculations. Note: the radial coefficients are divided by 4π, so that the V_{0000} term represents the isotropic potential.

extended to 9D using a new set of CCSD(T) calculations. The resulting 9D PES contains all relevant information to describe the interaction of all H_2O–H_2 isotopologues in zero-point or excited vibrational states. This 9D PES is subsequently averaged over the ground vibrational state of H_2O and H_2 in order to obtain the final average 5D CCSDT(T)-R12 PES. This latter 5D PES involves a conservative angular expansion over 149 angular functions $T_{p_1q_1p_2p}(\Theta, \Phi, \Theta', \Phi', \alpha, \beta, \gamma)$ (according to the conventions in Phillips et al. (1994)). A subset of 83 functions was selected, see Table 1, using a self-consistent Monte Carlo estimator and was checked to be sufficient for scattering calculations (see details below).

Figure 1 gives a comparison of the leading radial coefficients from Phillips et al. (1994) with the corresponding terms from the PES of Faure et al. (2005a). Faure et al.'s terms V_{1203} and V_{2224} are more repulsive by a few cm^{-1}, their isotropic V_{0000} term is deeper by about 10 cm^{-1} with a slight shift in the minimum, their V_{2024} term is smoother pointing to an expansion problem in Phillips et al.'s PES.

2.1. Influence of PES on cross sections

In order to probe the influence of the various PES on the scattering results, the rotational state-to-state cross-sections are obtained with exactly the same methods, parameters and molecular basis set sizes as in Dubernet & Grosjean (2002) and Grosjean et al. (2003).

The PES tests are first carried out on the excitation cross sections of ortho-water with para-H_2($j = 0$), at total energies chosen in the energy range necessary to get rate coefficients up to 20 K, i.e. at total energy of 90 cm^{-1}, 200 cm^{-1} and 410 cm^{-1}. At these total energies the number of open channels of ortho-H_2O is respectively 3, 6 and 14. All cross sections but those at 410 cm^{-1} and those among the 3 lowest transitions at 200 cm^{-1} are in the resonant regime.

Table 1. The 83 angular coefficients kept in the angular expansion of the potential energy surface of Faure et al. (2005a).

p_1	q_1	p_2	p	p_1	q_1	p_2	p	p_1	q_1	p_2	p	p_1	q_1	p_2	p	p_1	q_1	p_2	p
0	0	0	0	2	2	2	2	4	0	0	4	5	2	0	5	6	6	4	10
0	0	2	2	2	2	2	3	4	0	2	4	5	2	2	7	7	0	0	7
0	0	4	4	2	2	2	4	4	0	2	6	5	4	0	5	7	0	2	9
1	0	0	1	2	2	4	6	4	0	4	8	5	4	2	5	7	2	0	7
1	0	2	1	2	2	6	8	4	2	0	4	5	4	2	7	7	2	2	9
1	0	2	3	3	0	0	3	4	2	2	2	5	4	4	9	7	2	4	11
1	0	4	3	3	0	2	1	4	2	2	4	6	0	0	6	7	4	0	7
1	0	4	5	3	0	2	3	4	2	2	6	6	0	2	8	7	4	2	9
1	0	6	7	3	0	2	5	4	2	4	8	6	0	4	10	7	6	0	7
2	0	0	2	3	0	4	7	4	4	0	4	6	2	0	6	7	6	2	9
2	0	2	0	3	2	0	3	4	4	2	2	6	2	2	8	7	6	4	11
2	0	2	2	3	2	2	1	4	4	2	4	6	2	4	10	8	6	0	8
2	0	2	4	3	2	2	3	4	4	2	5	6	4	0	6	8	6	2	10
2	0	4	6	3	2	2	4	4	4	2	6	6	4	2	8	9	4	2	11
2	2	0	2	3	2	2	5	4	4	4	8	6	4	4	10	9	6	2	11
2	2	2	0	3	2	4	7	5	0	0	5	6	6	0	6				
2	2	2	1	3	2	6	9	5	0	2	7	6	6	2	8				

The tests aim to probe independently the influence of 3 features of the average 5D PES (Faure et al. 2005a): the number of terms kept in the angular expansion of the PES, the R12 correction and the vibrational corrections and at comparing these results with cross-sections calculated using the Phillips et al. (1994) PES. These detailed tests were not extended to rate coefficients, due to the cumbersome energy grid required to accurately reproduce the resonant structures in the cross-sections (Dubernet & Grosjean 2002).

For the three total energies we find that the 83 angular terms of Table 1 are sufficient to achieve an accuracy better than 0.1% on cross sections compared to using 149 angular functions; therefore all further tests and final rate calculations use 83 angular terms in the potential expansion.

Figure 2 compares the isotropic term of the H$_2$O-H$_2$ PES for the PES of Phillips et al. (1994) for steps 1, 2 and 3 of the PES of Faure et al. (2005a). Our CCSD(T) reference PES (step 1) is qualitatively similar to the MP4 PES of Phillips et al. (1994), and mostly differs by a fully converged radial and angular coverage. The R12 correction (step 2) is weakly anisotropic. It lowers the isotropic term by about 7 cm^{-1}, and changes the V_{1203} and V_{2224} terms in a similar fashion to the vibrational correction (step 3) from $R = 7$ a_0 to infinity; it has little effect both at short range for the V_{1203} and V_{2224} terms and for the V_{2024} term over the whole distance range. On the other hand the vibrational correction slightly deepens the isotropic term beyond $R = 7$ a_0 while it mostly affects the magnitude of all anisotropic terms at shorter range.

Figure 3 shows cross sections for the excitation of ortho-H$_2$O by para-H$_2(j = 0)$ obtained for the 4 levels of PES: (1) corresponds to the PES of Phillips et al. (1994); (2) corresponds to the 5D reference PES (Faure et al. 2005a) (step 1); (3) corresponds to step 2 where the R12 correction has been added; (4) gives the cross-section obtained with the full 5D-PES including the vibrational correction.

For the largest cross sections, differences from 1% to 15% occur between Phillips et al.'s PES (Phillips et al. 1994) and the 5D reference PES (Faure et al. 2005a) (step 1), the R12 correction (step 2) brings differences between 3% and 30% compared to the 5D reference PES, the effect decreasing with increasing energy. The vibrational correction (step 3) induces the largest difference, i.e. up to a factor of 2 with respect to the 5D reference PES at low energy and around 20–30% for the strongest
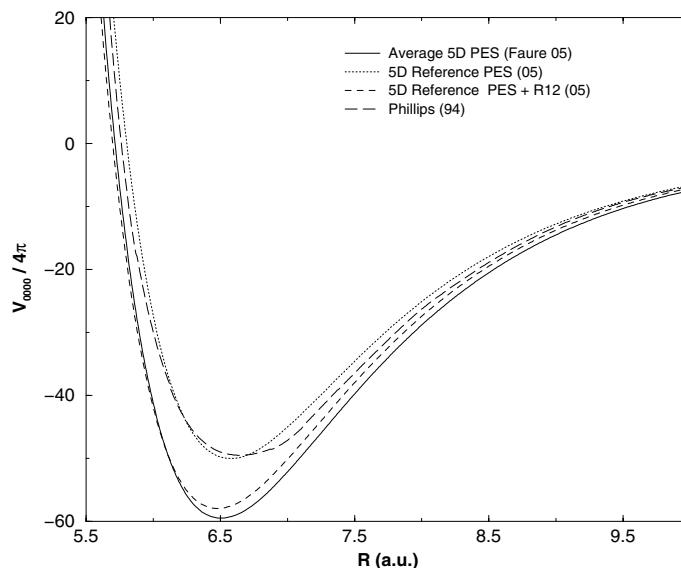

Fig. 2. Comparison of the isotropic H$_2$O–H$_2$ interaction terms ($V_{0000}/4\pi$ in cm^{-1}) for various PES: the solid line shows the final average 5D PES, the dotted line gives Phillips et al.'s PES (Phillips et al. 1994), the initial 5D reference PES (Faure et al. 2005a) (step 1) is represented by the long dashed line, and step 2 where the R12 correction has been added is given by the dashed line.

transitions at high energy. Overall the final average 5D PES (Faure et al. 2005a) induces differences in the largest cross sections of up to 40% at 410 cm^{-1}, up to 70% at 200 cm^{-1}, up to a factor 2 at 90 cm^{-1}. Away from the resonance region these large relative variations correspond to small absolute differences (about 1 Å^2) on small values of cross sections for collisions with para-H$_2(j = 0)$ as can be seen in Fig. 3.

The absolute differences found for collisions with ortho-H$_2(j = 1)$ are about the same order of magnitude, but excitation cross sections by ortho-H$_2(j = 1)$ are generally an order of magnitude larger than cross sections with para-H$_2(j = 0)$. Therefore the overall effect of the new PES on the excitation cross section with ortho-H$_2(j = 1)$ is not large. But it is found that at a total energy of 265 cm^{-1} and 321.706 cm^{-1} (equivalent respectively to 143.294 cm^{-1} and 200 cm^{-1} for para-H$_2(j = 0)$) both the R12 and the vibrational correction have a similar effect on
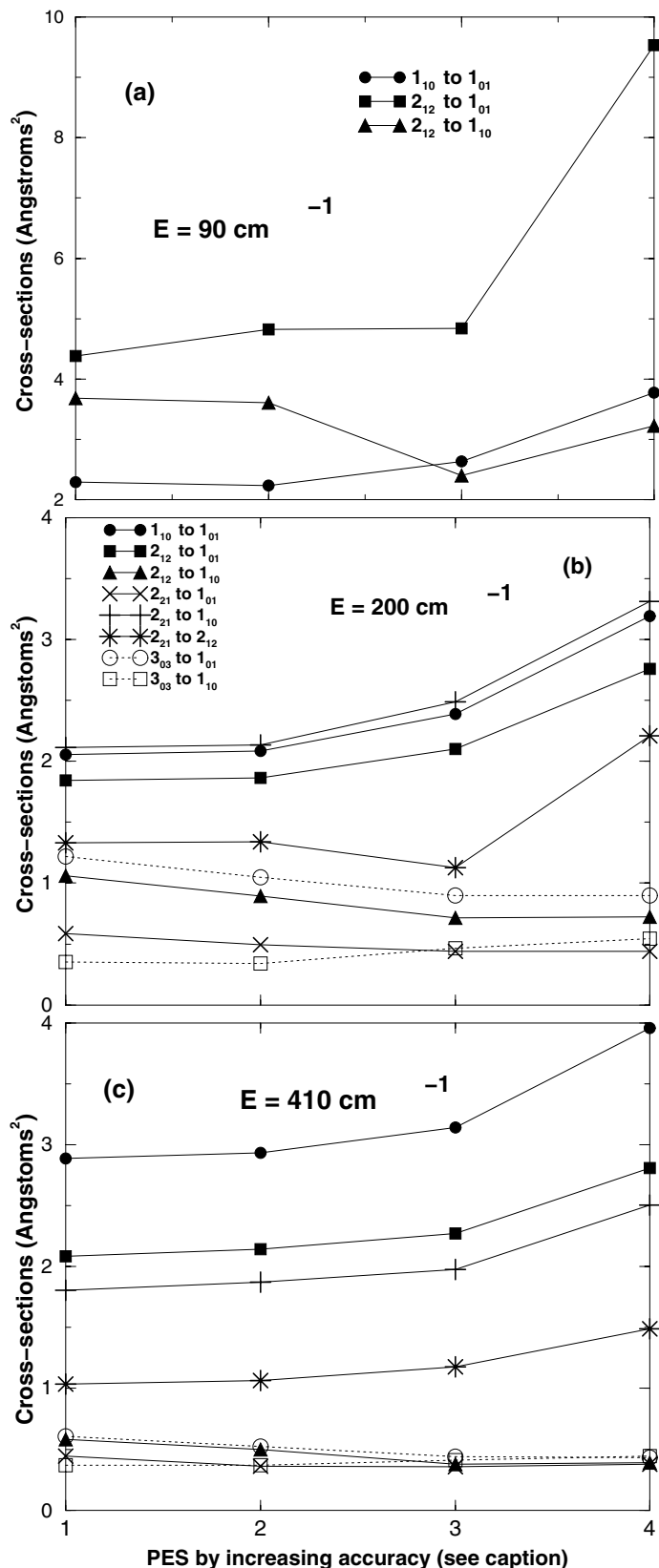
Fig. 3. Cross sections of the rotational excitation of ortho-H$_2$O by para-H$_2$($j = 0$) obtained at total energy of (a) 90 cm^{-1}, (b) 200 cm^{-1} and (c) 410 cm^{-1} for the 4 levels of PES by increasing accuracy: (1) is Phillips et al.'s PES (Phillips et al. 1994); (2) corresponds to the 5D reference PES (Faure et al. 2005a) (step 1); (3) corresponds to step 2 where the R12 correction has been added; (4) gives the cross-section obtained with the full PES including the vibrational correction.

excitation of cross sections of water by ortho-H$_2$($j = 1$). This is consistent with the fact that the two corrections change the anisotropic terms V_{1203}, V_{2224} in a similar way for the long range part of the potential. For collisions with para-H$_2$($j = 0$), there is no straightforward interpretation of the variation of the cross sections with the R12 and vibrational corrections because of the role of j(H$_2$) = 2 closed channels which account for about 20% to 30% of the cross sections. Nevertheless the generally stronger influence on cross section of the vibrational correction to the PES over the R12 correction seems to be related to the larger vibrationally corrected V_{1203}, V_{2224} and V_{2024} terms for $R < 7$ a_0.

2.2. Influence of PES on rate coefficients

In order to probe the influence of the new 5D PES (Faure et al. 2005a) we calculate rate coefficients for the excitation of ortho-H$_2$O with para-H$_2$($j = 0$) and ortho-H$_2$($j = 1$) from 5 K to 20 K, using the same scattering methods as in Dubernet & Grosjean (2002) and Grosjean et al. (2003).

Table 2 gives these rate coefficients at 20 K for some transitions, their ratios at 5 K, 10 K, 20 K with the Dubernet and co-workers rate coefficients (Dubernet & Grosjean 2002; Grosjean et al. 2003) (ratios (3)/(2)) and with Phillips et al. (1996) results (ratios (3)/(1)) and the ratios of the rate coefficients of Dubernet & Grosjean (2002); Grosjean et al. (2003) to those of Phillips et al. (1996) (ratios (2)/(1)).

The ratios (3)/(2) give the effect of using the new PES of Faure et al. (2005a) only, the ratios (2)/(1) show the difference induced by different dynamical calculations, while the ratios (3)/(1) include the effect of both the new PES (Faure et al. 2005a) and of the scattering calculations described elsewhere (Dubernet & Grosjean 2002; Grosjean et al. 2003). The rate coefficients for H$_2$O-para-H$_2$($j = 0$) presented in Dubernet & Grosjean (2002) were surprisingly different from those presented earlier by Phillips et al. (1996) at 20 K (in spite of using the same PES). In particular, the excitation rate coefficient for the 1_{01}–1_{10} transition of water was more than 50% larger than the Phillips et al. (1996) result. This was thought to be a consequence of an inadequately fine energy grid used by Phillips et al. (1996) in integrating cross-sections over a Maxwellian distribution of kinetic energies. The results of Grosjean et al. (2003) calculated between 5 K and 20 K for ortho-H$_2$($j = 1$) did not present any major difference at 20 K to the Phillips et al. (1996) results. These results are summarized by ratios (2)/(1) in Table 2.

We find that variations due to the PES can be as large as a factor 4 at 5 K for the de-excitation of the 1_{10} to 1_{01} transition by para-H$_2$($j = 0$), then decreasing to a factor 1.76 at 20 K. The (3)/(2) ratios of the transition 3_{03} to 2_{21} show similar behaviors with a factor of 2.74 at 5 K. For other transitions with para-H$_2$($j = 0$) the (3)/(2) ratios are not sensitive to temperature and are either increased by 80–100% or decreased by about 20%, noting that changes due to the PES do not occur uniformally among transitions.

Another feature is that collisions with ortho-H$_2$($j = 1$) are found to be much less sensitive to the PES than those with para-H$_2$($j = 0$). Due to the absence of the dipole-quadrupole coupling term, the cross sections involving para-H$_2$($j = 0$) are about an order of magnitude smaller, and are deeply affected by the strong resonance regime in the 5–20 K temperature range (Dubernet & Grosjean 2002). While the resonance regime is very sensitive to the details of the PES, strongly affecting the para-H$_2$($j = 0$) cross-sections and rates, it plays a smaller role in relative value for ortho-H$_2$($j = 1$), limiting the dependance of the ortho-H$_2$($j = 1$) rates on the PES. Consequently, the variations due to the new

Table 2. Ratios of de-excitation rates for ortho-H_2O colliding with para-($j = 0$) and ortho-H_2($j = 1$). Part a illustrates the effects at 20 K of an improved treatment of both scattering and PES (Col. (3)/(1)) and of the sole improvement of the scattering treatment (Col. (2)/(1)). The levels are labelled with $j_{K_{-1}K_1}$. The new rates are given for reference (Col. (3)) and slightly differ from the final rates in Table 3 by the collisional treatment (see text). Here (1) stands for calculations of Phillips et al. (1996); (2) for calculations of Dubernet at al. (2002) and Grosjean et al. (2003) using the same PES as in (1) and an improved treatment of scattering; and (3) for the present calculations using the new PES by Faure et al. (2005a) and the same treatment of scattering as in (2). Part b illustrates the influence of the sole PES at 5, 12 and 20 K. Conventions are similar to those of upper part.

Part (a)		Para-H_2($j = 0$)			Ortho-H_2($j = 1$)		
Initial	Final	(3)/(1)	(2)/(1)	(3)	(3)/(1)	(2)/(1)	(3)
				20 K			
$1_{1,0}$	$1_{0,1}$	2.85	1.62	3.34E-11	1.06	1.01	2.85E-10
$2_{1,2}$	$1_{0,1}$	1.67	1.06	3.38E-11	1.12	1.02	1.09E-10
$2_{1,2}$	$1_{1,0}$	0.95	1.08	1.60E-11	1.14	1.04	1.10E-10
$2_{2,1}$	$1_{0,1}$	0.75	1.01	3.23E-12	1.30	1.05	2.79E-11
$2_{2,1}$	$1_{1,0}$	1.59	1.01	3.30E-11	1.23	1.00	6.66E-11
$2_{2,1}$	$2_{1,2}$	2.12	1.12	1.87E-11	1.11	1.04	9.09E-11
$3_{0,3}$	$1_{0,1}$	0.86	1.02	7.32E-12	1.26	1.17	2.13E-11
$3_{0,3}$	$1_{1,0}$	1.60	0.98	6.06E-12	1.42	1.01	2.41E-11
$3_{0,3}$	$2_{1,2}$	1.56	0.90	3.45E-11	1.23	1.03	1.03E-10
$3_{0,3}$	$2_{2,1}$	1.96	1.12	4.43E-12	1.23	1.05	4.51E-11
Part (b)				ratio (3)/(2)			
		5 K	12 K	20 K	5 K	12 K	20 K
$1_{1,0}$	$1_{0,1}$	4.11	2.15	1.76	1.08	1.07	1.06
$2_{1,2}$	$1_{0,1}$	1.61	1.58	1.57	0.81	1.05	1.10
$2_{1,2}$	$1_{1,0}$	0.74	1.87	0.88	0.77	1.02	1.09
$2_{2,1}$	$1_{0,1}$	0.71	0.72	0.74	0.81	1.15	1.24
$2_{2,1}$	$1_{1,0}$	1.55	1.55	1.56	0.80	1.14	1.23
$2_{2,1}$	$2_{1,2}$	2.09	2.00	1.89	0.69	1.06	1.06
$3_{0,3}$	$1_{0,1}$	0.84	0.83	0.84	0.87	1.05	1.08
$3_{0,3}$	$1_{1,0}$	1.91	1.71	1.63	1.20	1.38	1.40
$3_{0,3}$	$2_{1,2}$	1.99	1.81	1.73	1.05	1.19	1.19
$3_{0,3}$	$2_{2,1}$	2.74	2.07	1.76	1.10	1.15	1.17

PES varies between a few and 40% for collisions with ortho-H_2($j = 1$) between 5 K and 20 K.

3. New rotational rate coefficients between 5 K and 20 K

For astrophysical applications a new set of effective de-excitation rate coefficients is now calculated using the average 5D PES of Faure et al. (2005a) and slightly improved scattering calculations compared to the procedure used in the previous sections and described in our previous publications (Dubernet & Grosjean 2002; Grosjean et al. 2003). We use close-coupling calculations for the whole energy range, the H_2 energy levels are now experimental energies (Dabrowski 1984) and the basis set for H_2O has been increased to $j_{H_2O} = 8$ with a cut-off procedure in energy in order to achieve better accuracy for the last 2 channels. This larger rotational basis set has no influence on the transitions previously considered by Dubernet & Grosjean (2002) and Grosjean et al. (2003). This can be verified by comparing the rate coefficients set (3) of Table 2 with the final rate coefficients of Table 3. The basis sets for para/ortho-H_2 still contain respectively $j(H_2) = 0, 2$ and $j(H_2) = 1, 3$. Extreme care was taken to reproduce all resonances correctly and to span the whole energy range necessary to obtain reliable rate coefficients up to 20 K.

Those effective rotational inelastic rate coefficients are given by the sum of the inelastic rate coefficients (Eq. (1)) over the final j_2' states for a given initial j_2:

$$\hat{R}_{j_2}(j\alpha \rightarrow j'\alpha')(T) = \sum_{j_2'} R(j\alpha, j_2 \rightarrow j'\alpha', j_2')(T), \qquad (1)$$

and the state-to-state rotational inelastic rate coefficients are the Boltzmann thermal averages of the inelastic cross sections:

$$R(\beta \rightarrow \beta')(T) = \left(\frac{8}{\pi\mu}\right)^{1/2} \frac{1}{(kT)^{3/2}} \int_0^\infty \sigma_{\beta \rightarrow \beta'}(E) E e^{-E/kT} dE, \qquad (2)$$

where $\beta \equiv j\alpha, j_2$ and $\beta' \equiv j'\alpha', j_2'$, unprimed and primed quantum numbers label initial and final states of the molecules, j and j_2 are the rotational angular momenta of H_2O and H_2 and α specifies the other H_2O quantum numbers (e.g. K_{-1}, K_1), E is the kinetic energy and k is the Boltzmann constant.

In the temperature range between 5 and 20 K, our effective rate coefficients follow the principle of detailed balance within the calculation error, because there are no transitions to the $j_2 = 3$ rotational level of ortho-H_2, and transitions to the $j_2 = 2$ rotational level of para-H_2 are negligeable. Therefore the excitation effective rate coefficients can be obtained by detailed balance using the energy levels given by Green et al. (1993) and listed in the BASECOL database (Dubernet et al. 2006). But in general only the $R(j\alpha, j_2 \rightarrow j'\alpha', j_2')$ and the $R(j\alpha \rightarrow j'\alpha')$ (rate coefficients summed over all final j_2' states and averaged over initial

Table 3. Effective de-excitation rate coefficients for Eq. (2) (in cm^{3}s^{-1}) for para-H$_2$O with para-H$_2$ ($j_2 = 0$) and ortho-H$_2$ ($j_2 = 1$). The levels are labelled with $j_{K_{-1}K_1}$. The levels are listed by increasing energy.

		Para-H$_2$O									
		$j_2 = 0$					$j_2 = 1$				
I	F	5	8	12	16	20	5	8	12	16	20
1_{11}	0_{00}	3.59E-11	3.40E-11	3.21E-11	3.07E-11	2.97E-11	1.11E-10	1.13E-10	1.15E-10	1.18E-10	1.20E-10
2_{02}	0_{00}	1.05E-11	1.11E-11	1.18E-11	1.22E-11	1.24E-11	2.62E-11	2.67E-11	2.74E-11	2.79E-11	2.83E-11
2_{02}	1_{11}	2.16E-11	2.25E-11	2.25E-11	2.21E-11	2.15E-11	1.56E-10	1.64E-10	1.71E-10	1.76E-10	1.79E-10
2_{11}	0_{00}	8.62E-14	1.83E-13	2.81E-13	3.38E-13	3.66E-13	9.04E-12	1.00E-11	1.07E-11	1.10E-11	1.12E-11
2_{11}	1_{11}	3.17E-11	3.64E-11	4.07E-11	4.31E-11	4.44E-11	8.94E-11	9.33E-11	9.72E-11	1.00E-10	1.03E-10
2_{11}	2_{02}	1.87E-11	1.93E-11	2.02E-11	2.11E-11	2.18E-11	1.63E-10	1.76E-10	1.90E-10	2.01E-10	2.09E-10
2_{20}	0_{00}	8.72E-13	9.58E-13	1.03E-12	1.07E-12	1.11E-12	9.61E-12	9.57E-12	9.61E-12	9.72E-12	9.86E-12
2_{20}	1_{11}	2.53E-11	2.57E-11	2.60E-11	2.61E-11	2.61E-11	5.40E-11	5.44E-11	5.55E-11	5.66E-11	5.78E-11
2_{20}	2_{02}	3.89E-12	4.15E-12	4.29E-12	4.34E-12	4.35E-12	3.71E-11	3.66E-11	3.61E-11	3.60E-11	3.60E-11
2_{20}	2_{11}	1.96E-11	2.03E-11	2.09E-11	2.13E-11	2.16E-11	1.26E-10	1.32E-10	1.39E-10	1.45E-10	1.50E-10
		Ortho-H$_2$O									
1_{10}	1_{01}	3.38E-11	3.42E-11	3.40E-11	3.37E-11	3.35E-11	2.35E-10	2.51E-10	2.67E-10	2.80E-10	2.89E-10
2_{12}	1_{01}	3.27E-11	3.26E-11	3.31E-11	3.36E-11	3.39E-11	6.21E-11	7.96E-11	9.32E-11	1.02E-10	1.09E-10
2_{12}	1_{10}	1.19E-11	1.30E-11	1.44E-11	1.54E-11	1.60E-11	6.54E-11	8.38E-11	9.71E-11	1.05E-10	1.10E-10
2_{21}	1_{01}	2.54E-12	2.74E-12	2.97E-12	3.13E-12	3.25E-12	1.64E-11	2.14E-11	2.47E-11	2.66E-11	2.79E-11
2_{21}	1_{10}	3.11E-11	3.19E-11	3.27E-11	3.30E-11	3.31E-11	3.84E-11	5.07E-11	5.89E-11	6.36E-11	6.66E-11
2_{21}	2_{12}	2.15E-11	2.07E-11	1.99E-11	1.93E-11	1.88E-11	4.62E-11	6.37E-11	7.72E-11	8.54E-11	9.09E-11
3_{03}	1_{01}	6.75E-12	6.90E-12	7.08E-12	7.23E-12	7.34E-12	1.66E-11	1.87E-11	2.01E-11	2.08E-11	2.14E-11
3_{03}	1_{10}	7.06E-12	6.77E-12	6.47E-12	6.24E-12	6.06E-12	2.15E-11	2.33E-11	2.40E-11	2.41E-11	2.41E-11
3_{03}	2_{12}	4.00E-11	3.86E-11	3.70E-11	3.57E-11	3.46E-11	7.33E-11	8.47E-11	9.35E-11	9.93E-11	1.03E-10
3_{03}	2_{21}	5.05E-12	5.12E-12	4.92E-12	4.68E-12	4.44E-12	3.16E-11	3.67E-11	4.11E-11	4.37E-11	4.51E-11

j_2 states) satisfy the usual detailed balance relations between forward and reverse rate coefficients, and the $\hat{R}_{j_2}(j\alpha \rightarrow j'\alpha')$ do not since they do not involve a complete thermal average (Phillips et al. 1996).

Tables 3 presents a sub-set of these new effective rate coefficients calculated among the lowest 10 levels of ortho-H$_2$O and para-H$_2$O owing to collisions with para-H$_2$($j = 0$) and ortho-H$_2$($j = 1$) at kinetic temperatures ranging from 5 to 20 K. The full set of effective rate coefficients, state-to-state rate coefficients and energy levels used in the calculations can be retrieved from the BASECOL database (Dubernet et al. 2006) or obtained on request from one of the authors (MLD). The BASECOL database (Dubernet et al. 2006) also provides Einstein coefficients taken from either the JPL (Pickett et al. 1998) or the CDMS (Müller et al. 2005) catalogs. The labelling of transitions for the Einstein coefficients is consistant with the labelling of energy levels and rate coefficients.

4. Concluding remarks

A new average 5D potential energy surface has been used to calculate new collisional de-excitation rate coefficients for the lowest 10 levels of ortho and para-water in collision with ortho ($j = 1$) and para-H$_2$($j = 0$) for kinetic temperatures from 5 to 20 K. The new PES of Faure et al. (2005a) leads to a significant re-evaluation of the rate coefficients for the excitation of H$_2$O by para-H$_2$($j = 0$). Indeed for the 1_{10} to 1_{01} transition observed by the SWAS satellite, the new PES increases the de-excitation rate coefficient by a factor of 4 at 5 K and by 75% at 20 K compared to the previous results of Dubernet et al. (Dubernet & Grosjean 2002; Grosjean et al. 2003), leading to a total increase at 20 K of 185% with respect to the Phillips et al. (1996) results. The de-excitation rate coefficients of other transitions induced by para-H$_2$ can increase by as much as 100% or decrease by 30%. For collision with ortho-H$_2$($j = 1$) the new PES has a smaller effect on the de-excitation rate coefficients: a maximum change of 40%.

Although fairly accurate, the present 5D PES may still deviate from the CCSD(T) limit by about 1–2 cm^{-1} and has no provision for high excitations beyond the CCSD(T) limit. Recent investigation of CO–H$_2$ interactions by Noga et al. (2006) indicate that the missing triple and quadruple excitations lower the absolute minimum by about 3 cm^{-1} and change the anisotropic behaviour. However the CO molecule, with its triple bond and small dipole, might be an extreme case in this respect. The implications of such minor PES inaccuracies for the low temperature H$_2$–H$_2$O rates is hard to estimate.

Our next goal is to obtain the best possible accuracy for the whole temperature range up to 500 K and for all levels of interest, using close coupling and coupled states methods. Quasi classical calculations are also feasible and provide a fair agreement with quantal calculations down to 100 K (Faure et al. 2006). However they are unreliable for estimating the smallest rates, i.e. below 10^{-11} cm^3 s^{-1}, and quantal calculations therefore are preferred.

Higher temperature, up to 1000 K, rotational rate coefficients will also be obtained using IOS calculations checked against coupled states calculations, and will be compared with vibrational close coupling-IOS (VCC-IOS) calculations in order to test the influence of the first bending state of water.

References

Cernicharo, J., & Crovisier, J. 2005, Space Sci. Rev., 119, 29

Cernicharo, J., Goicoechea, J. R., Daniel, F., et al. 2006, ApJ, 649, L33

Dabrowski, I. 1984, Can. J. Phys., 62, 1639

Daniel, F., Dubernet, M.-L., & Meuwly, M. 2004, J. Chem. Phys., 121, 4540

Daniel, F., Cernicharo, J., & Dubernet, M.-L. 2005a, in IAU Symp., 163

Daniel, F., Dubernet, M.-L., Meuwly, M., Cernicharo, J., & Pagani, L. 2005b, MNRAS, 363, 1083

Daniel, F., Cernicharo, J., & Dubernet, M.-L. 2006, ApJ, 648, 461

Dubernet, M., Grosjean, A., Daniel, F., et al. 2006, in Ro-vibrational Collisional Excitation Database: BASECOL, `http://www.obspm.fr/basecol` (Japan: Special Issue of the Journal of Plasma and Fusion Research, series 7, in press)

Dubernet, M. L. 2005, in IAU Symp., 235

Dubernet, M.-L., & Grosjean, A. 2002, A&A, 390, 793

Faure, A., Valiron, P., Wernli, M., et al. 2005a, J. Chem. Phys., 122, 221102

Faure, A., Wiesenfeld, L., Wernli, M., & Valiron, P. 2005b, J. Chem. Phys., 123, 104309

Faure, A., Wiesenfeld, L., Wernli, M., & Valiron, P. 2006, J. Chem. Phys., in press

Green, S. 1980, ApJS, 42, 103

Green, S., Maluendes, S., & McLean, A. D. 1993, ApJS, 85, 181

Grosjean, A., Dubernet, M.-L., & Ceccarelli, C. 2003, A&A, 408, 1197

Lique, F., & Cernicharo, J. 2006, in private communication

Lique, F., Spielfiedel, A., Dubernet, M.-L., & Feautrier, N. 2005, J. Chem. Phys., 123, 4316

Maluendes, S., McLean, A. D., & Green, S. 1992, J. Chem. Phys., 96, 8150

Melnick, G. J., Stauffer, J. R., Ashby, M. L. N., et al. 2000, ApJ, 539, L77

Müller, H. S. P., Schlöder, F., Stutzki, J., & Winnewisser, G. 2005, Journal of Molecular Structure, 742, 215

Noga, J., & Kutzelnigg, W. 1994, J. Chem. Phys., 101, 7738

Noga, J., Kallay, M., & Valiron, P. 2006, Molecular Phys., accepted

Palma, A., Green, S., Defrees, D. J., & McLean, A. D. 1988a, ApJS, 68, 287

Palma, A., Green, S., Defrees, D. J., & McLean, A. D. 1988b, J. Chem. Phys., 89, 1401

Palma, A., Green, S., Defrees, D. J., & McLean, A. D. 1989, ApJS, 70, 681

Phillips, T. R., Maluendes, S., McLean, A. D., & Green, S. 1994, J. Chem. Phys., 101, 5824

Phillips, T. R., Maluendes, S., & Green, S. 1996, ApJS, 107, 467

Pickett, H. M., Poynter, R. L., Cohen, E. A., et al. 1998, J. Quant. Spectrosc. Rad. Trans., 60, 883

Sandqvist, A., Bergman, P., Black, J. H., et al. 2003, A&A, 402, L63

Spinoglio, L., Codella, C., Benedettini, M., et al. 2001, The Promise of the Herschel Space Observatory, ed. G. L. Pilbratt, J. Cernicharo, A. M. Heras, T. Prusti, & R. Harris, ESA-SP, 460, 495

Tsuji, T. 2001, A&A, 376, L1

Wilson, C. D., Mason, A., Gregersen, E., et al. 2003, A&A, 402, L59

Wright, C. M., vanDishoeck, E. F., Black, J. H., et al. 2000, A&A, 358, 689